Iraqi Journal of Natural Sciences and Nanotechnology 7(1) (2026) 117-132

Iraqi Journal of Natural Sciences and Nanotechnology IJNSN

Monte Carlo Simulation in Extensive Air Showers for Ultra- High Energies

Kadhom F. Fadhel

Directorate General of Education in Diyala, Ministry of Education, Baghdad, Iraq

Corresponding Author : kadhumfakhry@uomustansiriyah.edu.iq

Keywords:

lateral distribution function;
Universal Cosmic Rays;
Extensive Air Showers;
Aires;
CORSIKA code;

Abstract

In the present work, two simulation models AIRES Version 19.04.00 and CORSIKA5.62 code will be used to simulate the lateral distribution function (LDF) of the Cherenkov photon flux in the Extensive Air Showers (EAS). The simulation was performed using the high-energy hadronic interaction QGSJET98 model with the Haverah Park array. Two primary particles oxygen and proton with energies between 1015 and 1019 eV were simulated at various zenith angles like (0˚, 20˚, and 45˚). Depending on the Quick Fit function a parameterization of the density of the shower as a function of primary energy was reconstructed based on this simulation for primary proton and oxygen at several zenith angles. A comparison between the simulation Cherenkov photon flux LDF for primary proton and oxygen by Haverah Park, and a comparison of the calculated parameterization of the density of the shower measured on the Tunka EAS array. The light emitted in the shower propagated and attenuated to the ground, the exponential function is suitable to use for developing an EAS. Through four parameters as a function of primary energy in the knee and ankle portions of the cosmic ray spectrum, the EAS array offers the chance to identify the particle responsible for the shower and determine its energy. For primary oxygen and proton, the extrapolation of approximate Cherenkov photon flux LDF for high energies was found.

Introduction

Investigating the traits of EAS produced by Cosmic Rays (CRs) with extremely high energies is essential. In addition, the chain reaction EAS showers that are generated in the atmosphere surrounding the Earth have been used to detect high-energy cosmic rays. Since some primary particles are not observable immediately. Consequently, they need to be looked into based on the showers that were measured in various ways. Due to their incredibly low fluxes, the Ultra High Energy Cosmic Rays (UHECR) that reach the Earth cannot be directly observed in space [1].

These particles interact with atomic nuclei as they enter the atmosphere, causing secondary particles known as EAS. There are millions of collisions and secondary particle decays in the EAS. These showers can be seen with detectors, which can track energy depositions as they grow along the atmosphere, or surface detectors, which track depositions as the particles hit the ground [2]. One of the main EAS aspects that large ground-based air shower arrays are able to monitor with exceptional accuracy at different distances from the shower core is the local density of charged particles [3]. The only reliable way to determine a CR basic energy spectrum, composition, and testing hadronic interaction models at superhigh energies is to compare experimental data with the outcomes of EAS simulations. As a result, precise theoretical forecasts of the lateral distribution function (LDF) of the fundamental EAS elements at a variety of distances from the shower are essential for both interpreting previous experimental results and studying the design of future experiments in CR research [4,5]. Studying the energy spectrum and mass composition of primary cosmic rays in the energy range between 10^{13} to 10^{17} eV is of special interest in light of the observed index change of the power spectrum of the Primary Cosmic Radiation (PCR) spectra close to 3PeV, referred to as the "knee" region [6]. Cherenkov radiation, which is released by relativistic cosmic rays in the EAS, provides crucial information regarding the development of the shower and PCR particles. The Cherenkov light LDF depends on the energy and primary particle type, observation level, height of the first collision, and direction of the shower axis [7]. One of the essential instruments of numerical simulation for investigating EAS characteristics and processing and analyzing experimental data is the Monte Carlo method, which can be used to determine the primary particle energy type and shower axis from the characteristics of Cherenkov photon flux of secondary charged particles [8,9] have offered thorough explanations of the simulation, experimental setup, and Cherenkov light detection method in EAS. As G. R. Farrar and H.-J. Drescher, [10] the Cherenkov photon flux LDF generated throughout the shower growth phase was measured using electrons with energy ranging from 8 to 200 GeV. Comparison of the Cherenkov photon flux profiles and the results of Monte Carlo simulations is discussed. Mavrodiev et al. 3Pev [11] have installed the LDF of EAS array Tunka-133. This array enables a systematic analysis of the mass composition and energy spectrum of cosmic rays in the energy range 1016–10^{18} eV. The depth of the EAS maximum Xmax might be determined by analyzing the LDF and time structure of the EAS Cherenkov photon flux [12,13]. In the current work, two models AIRES [14] and CORSIKA code [15] for simulation of hadronic processes, which is QGSJET for simulation of the EAS are used to simulate LDF for circumstances and configurations of the Haverah Park EAS array [16]. On the basis of Quick Fit function, a method for describing the lateral distribution of the showers, the results of the numerical simulation of LDF density were approximated, and its potential for use in reconstructing the events recorded in Haverah Park was examined. The primary benefit of this strategy is the ability to recapture LDF events that were observed using the Haverah Park array. Located 500 meters apart, the four 34 m^2 water-Cherenkov detectors (A1–A4) make up the core portion of the Haverah Park array. In order to obtain density data from every location for showers that activate the 500 m array, six sets of satellite arrays, each measuring 4 × 14 m^2, are located close to a radius of 2 km around the center. Above $\approx 6 \times 10^{16}$ eV, showers with primary energy are sensitive to the 500 m array. A 150 m array of three additional detectors, each measuring 9 m2, surrounds the primary detector (A1). The so-called infill array is made up of 23 small-area water-Cherenkov detectors spaced irregularly at intervals of around 150

meters in the center of the 500-meter array. In contrast, the Tunka-133 array has 133 wide-angle optical detectors with a 20 cm diameter hemispherical photocathode that are based on the PMT EMI 9350. The detectors are placed into 19 clusters, with seven detectors each cluster, including one in the middle and six in a hexagonal pattern. Within the cluster, the detectors are 85 meters apart. A good chance for primary particle identification and the characterization of its energy around the knee and ankle areas has been demonstrated by comparing the approximated LDF with the reconstructed showers recorded with Tunka-133 [17].

Lateral Distribution of Atmospheric Cherenkov Light

In this work, the QGSJET model for interactions of hadrons with energy larger than 80 GeV is used to simulate the evolution of the atmospheric cascade and the lateral dispersion of Cherenkov photon flux in EAS [18]. The interactions and decay of different nuclei, photons, hadrons, electrons, and muons in the atmosphere are simulated using the AIRES and CORSIKA code [19]. The particles are observed as they move through the atmosphere until they interact with an air nucleus or, in the case of secondary particles that are unstable, until they decay [20]. Details about the arrival time, type, location, momentum, and energy of the created secondary particles at a chosen altitude above sea level are included in the simulation results [21]. For hadronic cascades with energy in the "knee" and "ankle" regions, the atmosphere was predicted to be near the shower maximum in the simulation at this observation level. The simulations are able to provide flatter distributions of the different shower components, particularly the flux of atmospheric Cherenkov photons, because the changes in shower development are less noticeable than at lower observation levels [22]. Protons as well as oxygen act as the primary nuclei that start the simulation of LDF flux densities in EAS. The acquired lateral distribution of Cherenkov photon flux densities in EAS with less uncertainty leads to a significant reduction of statistical fluctuations. The LDF in EAS created by primary protons with a vertical shower and an energy range of 1015–1019 eV is shown in Figures 1 and 2 using simulation software AIRES and CORSIKA code. The measured lateral distributions of atmospheric LDF caused by various cosmic ray nuclei around the "knee" and "ankle" regions. Where the axis shows 'R' the distance from the shower axis, while the vertical axis 'Q' represents the number of particles resulting from the interaction of cosmic ray particles with the atmospheric particles. We notice that the simulation curves begin to increase as the energy of the incident particle increases. This means that the number of secondary particles produced from the interaction increases as the energy of the incident particle increases. A comparison of the lateral distribution of Cherenkov photon flux for different primary energies like (3×1015 and 3×1018) eV using AIRES and CORSIKA code for primary oxygen as well as proton is shown in Figures 3 and 4 for several zenith angles ($\theta = 0^{\circ}$, 20°, and 45°). The shower's development-related variations predominate in the high-energy range over 1015 eV. Figure 4 shown the comparison between AIRES and CORSIKA simulation for LDF of Cherenkov photon flux by two primary particles (oxygen and proton) at energies (3×1015 and 3×1018) eV. Through the figures, we conclude that

the simulation curves begin to decrease as the azimuth angle of the incident body increases. This means that when a particle incident vertically, it travels a longer path to produce secondary particles than the particle that occurs at a certain angle, and the path of the particle decreases as the angle of incidence increases.

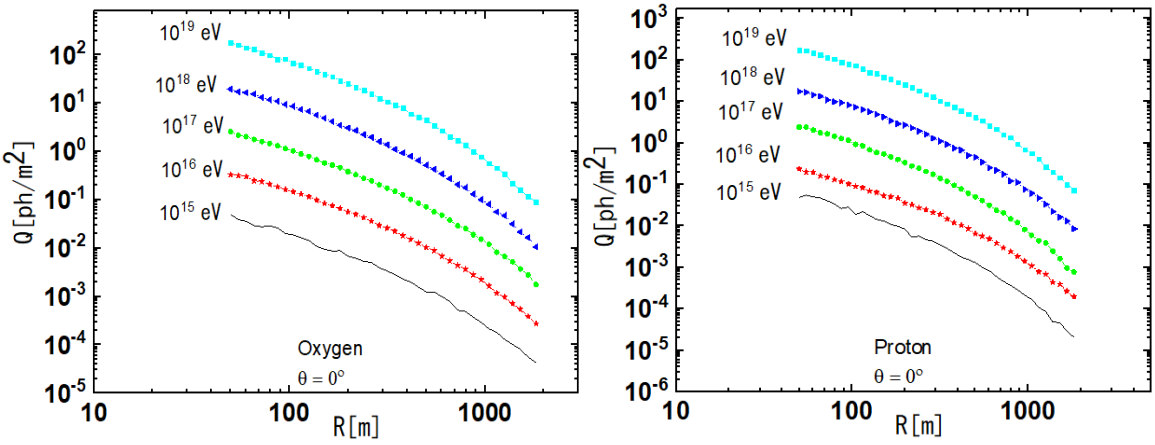

Figure 1: The primary energies effect of LDF by primary (oxygen and proton) using AIRES code for vertical showers.

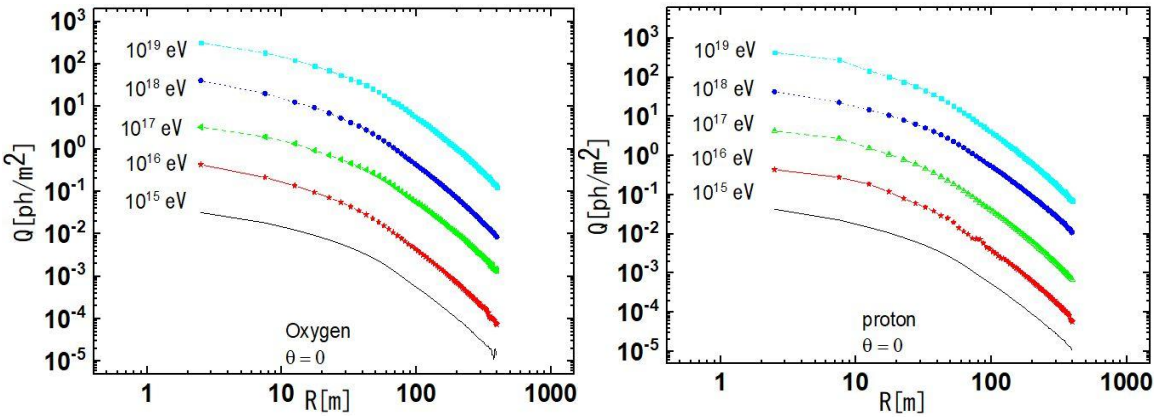

Figure 2: The primary energies effect of LDF by primary (oxygen and proton) using CORSIKA code for vertical showers.

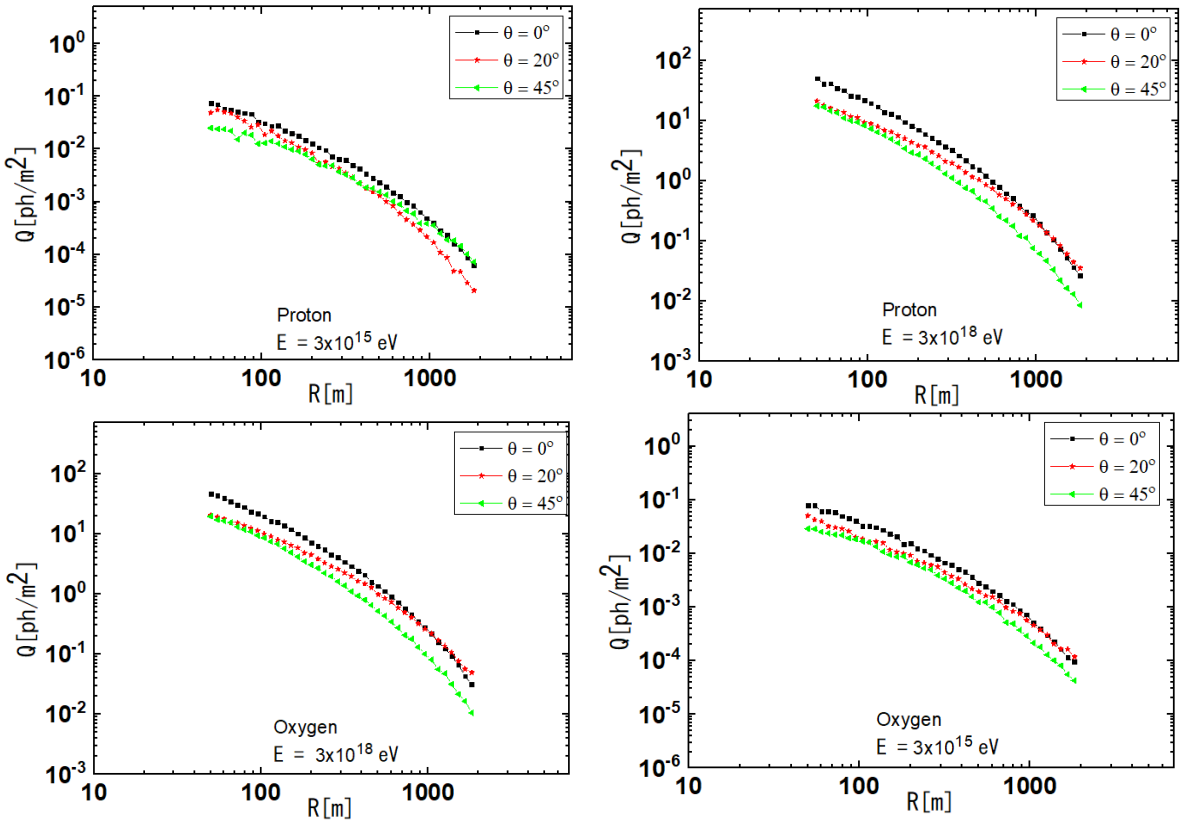

Figure 3: The zenith angle effects of LDF by primary (oxygen and proton) using AIRES code at the primary energies (3×10^{15} and 3×10^{18}) eV.

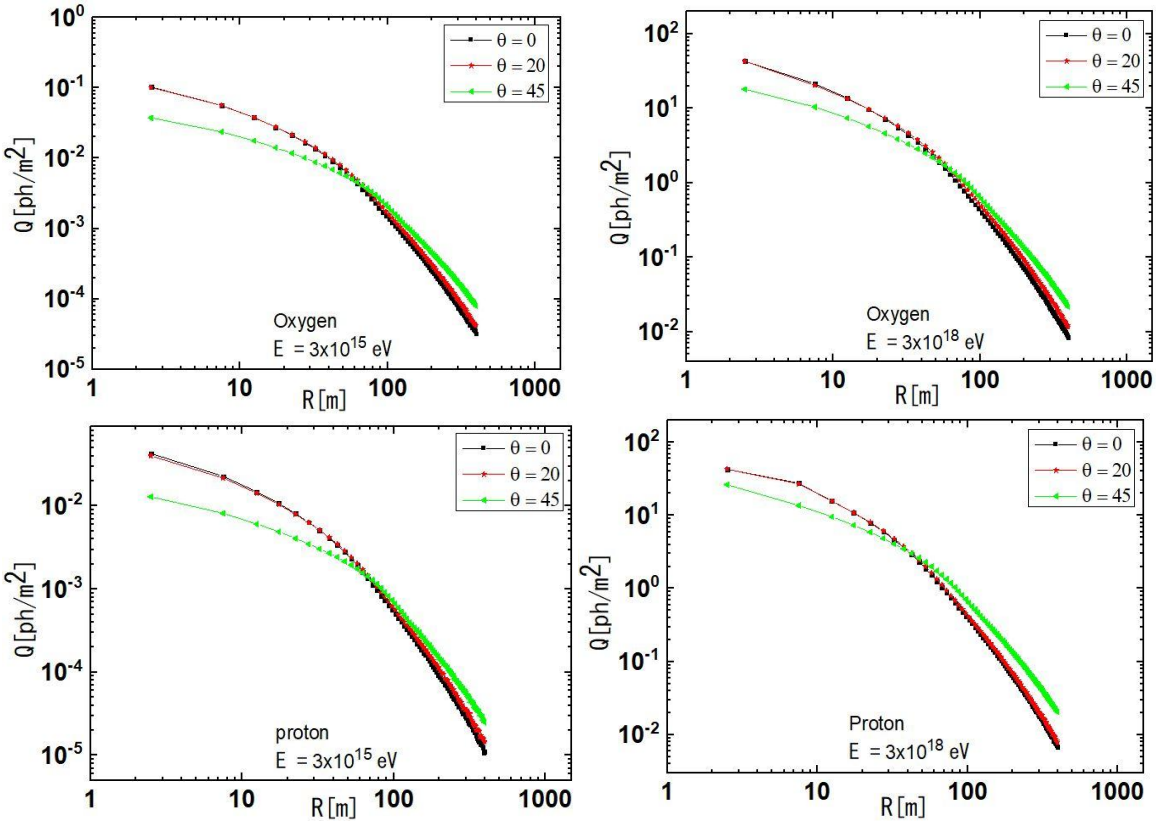

Figure 4: The zenith angle effects of LDF by primary (oxygen and proton) using CORSIKA code with the two primary energies (3×10^{15} and 3×10^{18}) eV.

Parameterization of the Lateral Distribution and Event Reconstruction

The flux of Cherenkov photon in order to learn more about primary particles, event reconstruction often uses the LDF function to describe how photon of Cherenkov flux varies laterally with core distance. The shower density, or overall number of particles, is obtained by integrating throughout the entire range of the LDF core distance. The total number of photon Cherenkov flux (N_γ) emitted by electrons in the EAS, which is directly proportional to the primary energy E_0, is also used to estimate the parameter as follow [23]:

$$N_\gamma(E_0) \approx 3.7 \times 10^3 \frac{E_0}{\xi_e} \approx 4.5 \times 10^{10} \frac{E_0}{10^{15} eV} \qquad (1)$$

where ξe is equal to 81.4MeV, critical energy for electrons. Since it is challenging to determine this magnitude experimentally, Cherenkov photon flux density, or the number of photons ($\Delta N\ \gamma$) per unit detector area (ΔS), which varies with distance from the shower axis and energy, can be used [24]:

$$Q(R) = \frac{\Delta N_\gamma(R)}{\Delta S} \qquad (2)$$

where *R* is the radius around the shower axis. Direct observations of Cherenkov light show that the variation of LDF in EAS is fundamentally less than the total amount of photons N_γ [25]. The High Energy Cosmic Ray Experiment HECRE proposed parameterization [26].

$$Q(R) = \frac{\sigma e^{\alpha}\, e^{-[(\frac{R}{\gamma})+(R-r_0/\gamma)+(R/\gamma)^2+\frac{(R-r_0)^2}{\gamma^2}]}}{\gamma[(R/\gamma)^2-\frac{(R-r_0)^2}{\gamma^2}+\frac{R\sigma^2}{\gamma}]} \qquad (3)$$

where *R* is the separation from the shower axis, and the model parameters are *s*, *g*, *a* and *r0* According to the model, the total number of Cerenkov photons at the specified observation level multiplied by a parameter equals the energy of the incident primary particle.

$$\beta = (R/\gamma)^2 + \frac{(R-r_0)^2}{b^2} \qquad (4)$$

$$S = \gamma[(R/\gamma)^2 - \frac{(R-r_0)^2}{\gamma^2} + \frac{R\sigma^2}{\gamma}] \qquad (5)$$

Substituting equation (4) and equation (5) into (3), we get.

$$Q(R) = \frac{\sigma e^{\alpha}\, e^{-[(\frac{R}{\gamma})+(R-r_0/\gamma)+\beta]}}{S} \qquad (6)$$

From equation Quick fit (Logistic model) for AIRES data.

$$Q_{A(M)} = \frac{\xi_1-\xi_2}{1+(\frac{X}{X_0})^\eta} + \xi_1 (7)$$

We utilized the proposed function for the Cherenkov photon flux LDF, which depends on several sets of shower simulations using different parameters $\xi_1, \xi_2, X_{0,}$ and η as a function of the primary mass, (show Table 1). Fitting the AIRES code yields these coefficients, which are provided by the polynomial form:

$$K_{A(M)} = C_0 + C_1 \lg(E_0) + C_2 \lg(E_0)^2 + C_3 \lg (E_0)^3 \qquad (8)$$

where $K_{A(M)} = \xi_1, \xi_2, X_{0,}$ and η are several sets of shower parameters of Eq. (7) as a function of the primary mass and C_0, C_1, C_2, and C_3 are their coefficients (show Table 1).

From equation Quick fit (Logistic model) for CORSIKA data.

$$Q_{C(M)} = \frac{\xi_1 - \xi_2}{1+(\frac{X}{X_0})^{\eta}} + \xi_1 \qquad (9)$$

We utilized the proposed function for the Cherenkov photon flux LDF, which depends on several sets of shower simulations using different parameters ξ_1, ξ_2, X_0, and η as a function of the primary mass, (show Table 2). Fitting the CORSIKA code yields these coefficients, which are provided by the polynomial form:

$$K_{C(M)} = C_0 + C_1 \lg(E_0) + C_2 \lg(E_0)^2 + C_3 \lg (E_0)^3 \qquad (10)$$

where $K_{C(M)} = \xi_1, \xi_2, X_0$, and η are several sets of shower parameters of Eq. (9) as a function of the primary mass and C_0, C_1, C_2, and C_3 are their coefficients (show Table 2).

Table (1) the coefficients of the exponential function (Eq. 7) for the specified energy range can be determined by using the parameterized AIRES code simulation for the different primaries within the energy range (10^{15}-10^{19}) eV and different zenith angles (0˚, 20˚, and 45˚).

Primary particles	$(\theta)^{\circ}$	$K_{A(M)}eV$	Coefficients			
			C_0	C_1	C_2	C_3
Proton	0˚	η	303264.77	7.007×10^{-12}	-9.18×10^{-31}	-1.97103×10^{-17}
		ξ_1	-2.53×10^{6}	5.73×10^{-10}	3.25×10^{-30}	-4.345×10^{-18}
		ξ_2	360.83	6.47×10^{-17}	-4.7×10^{-36}	2.274×10^{-20}
		X_0	46.5	1.14×10^{-17}	-8.1×10^{-37}	-1.344×10^{-15}
	20˚	η	280192.9	3.71×10^{-12}	-5.02×10^{-31}	-4.76×10^{-16}
		ξ_1	-1.57×10^{6}	3.62×10^{-10}	1.97×10^{-30}	-2.129×10^{-16}
		ξ_2	365.006	6.4×10^{-17}	-4.64×10^{-36}	-8.36×10^{-19}
		X_0	46.87	1.19×10^{-17}	-8.58×10^{-37}	2.246×10^{-17}

	45˚	η	- 4919.06	-1.89×10^{-13}	9.21×10^{-33}	8.55×10^{-18}
		ξ_1	32094.02	4.97×10^{-12}	-1.5×10^{-31}	-1.95×10^{-16}
		ξ_2	347.37	7.96×10^{-17}	-6.19×10^{-36}	-8.74×10^{-19}
		X_0	97.77	1.54×10^{-17}	-1.3×10^{-36}	1.39×10^{-15}
Oxygen	0˚	η	5916.11	-4.93×10^{-13}	2.51×10^{-32}	-2.728×10^{-17}
		ξ_1	62389.11	9.92×10^{-12}	-2.92×10^{-31}	-3.058×10^{-18}
		ξ_2	350.56	7.24×10^{-17}	-5.52×10^{-36}	2.47×10^{-20}
		X_0	96.56	2.2×10^{-17}	-1.9×10^{-36}	8.36×10^{-16}
	20˚	η	399198.83	4.1×10^{-12}	-4.25×10^{-31}	-2.37×10^{-17}
		ξ_1	-6.9×10^{6}	5.5×10^{-10}	2.42×10^{-30}	1.53×10^{-17}
		ξ_2	338.23	8.78×10^{-17}	-7.38×10^{-36}	9.97×10^{-18}
		X_0	48.09	8.27×10^{-18}	-6.2×10^{-37}	2.27×10^{-18}
	45˚	η	253138.19	2.48×10^{-12}	-2.53×10^{-31}	1.852×10^{-16}
		ξ_1	-4.26×10^{6}	3.48×10^{-10}	1.52×10^{-30}	$-3.99327\text{x}10^{-18}$
		ξ_2	341.67	8.77×10^{-17}	-7.37×10^{-36}	1.97×10^{-17}
		X_0	48.63	8.15×10^{-18}	-6.09×10^{-37}	6.117×10^{-18}

Table (2) one may determine the coefficients of the exponential function (Eq. 9) for the specified energy range by using the parameterized CORSIKA code simulation for the different primaries within the energy range (10^{15}-10^{19}) eV and with different zenith angles (0˚, 20˚, and 45˚)

Primary particles	$(\theta)^{\circ}$	$K_{C(M)}eV$	Coefficients			
			C_0	C_1	C_2	C_3
Proton	0˚	η	612.9414	-1.13×10^{-37}	2.27×10^{-18}	-1.64×10^{-36}
		ξ_1	618.40936	-1.06×10^{-34}	1.852×10^{-16}	-1.61×10^{-38}
		ξ_2	708.23353	-4.15×10^{-37}	$-3.99327\text{x}10^{-18}$	2.95×10^{-35}
		X_0	602.56899	5.8×10^{-35}	1.97×10^{-17}	-3.92×10^{-37}
	20˚	η	599.09638	-3.6×10^{-37}	6.117×10^{-18}	-6.026×10^{-36}
		ξ_1	604.14023	-2.39×10^{-37}	5.74×10^{-17}	-3.94×10^{-38}
		ξ_2	698.51376	3.58×10^{-39}	-6.719×10^{-19}	-2.45×10^{-37}
		X_0	677.89985	4.81×10^{-35}	1.218×10^{-15}	-7.05×10^{-38}
	45˚	η	659.88262	-1.56×10^{-36}	-2.105×10^{-17}	3.03×10^{-36}
		ξ_1	630.47672	-9.9×10^{-36}	1.539×10^{-17}	3.075×10^{-37}
		ξ_2	730.08085	-3.61×10^{-38}	1.74×10^{-19}	$-4.563\text{ x}10^{-37}$

		X_0	638.24296	8.76×10^{-37}	6.319×10^{-16}	-2.19×10^{-37}
Oxygen	0˚	η	596.05846	-1.48×10^{-36}	-1.09×10^{-17}	9.159×10^{-36}
		ξ_1	584.02586	-3.24×10^{-34}	6.23×10^{-17}	5.93×10^{-38}
		ξ_2	686.10838	5.62×10^{-37}	4.267×10^{-19}	-2.052×10^{-36}
		X_0	644.98568	1.102×10^{-33}	1.312×10^{-17}	-5.13×10^{-39}
	20˚	η	614.05591	-9.823×10^{-37}	4.166×10^{-18}	-2.52×10^{-37}
		ξ_1	618.61098	3.019×10^{-16}	$-1.05203\text{x}10^{-38}$	7.25×10^{-37}
		ξ_2	808.26112	-2.007×10^{-17}	2.85×10^{-35}	-1.69×10^{-36}
		X_0	673.83563	9.973×10^{-17}	1.01×10^{-36}	-1.65×10^{-38}
	45˚	η	691.89401	3.75×10^{-19}	-2.052×10^{-36}	-2.195×10^{-37}
		ξ_1	616.04302	-2.96×10^{-18}	-5.13×10^{-39}	-1.89×10^{-37}
		ξ_2	806.51739	2.53×10^{-17}	-2.52×10^{-37}	1.61×10^{-35}
		X_0	665.61695	3.282×10^{-15}	7.135×10^{-38}	-1.57×10^{-37}

Comparison of the Approximated LDF with AIRES and CORSIKA

The resultant simulation of Cherenkov photon flux LDF exhibits, in agreement with previous simulation models AIRES and CORSIKA code. The parameterized Cherenkov photon flux LDF that was obtained by Eq. 7 and 9 (quick function) was compared with the AIRES and CORSIKA

code simulation for the energy spectrum of cosmic rays. This study revealed good agreement between the range of fundamental energies (10^{15}, 10^{16}, and 10^{19}) eV for vertical showers and the beginning proton primary particle. Figures 5 and 6 show the parameterization of the Cherenkov photon flux in EAS as a function of the primary mass using (Eq.7 and 9) the Quick fit function, by two simulation models AIRES and CORSIKA code for two primary energies the first energy (3×10^{15} eV) is the knee region spectrum of (CR) and the second energy (3×10^{18} eV) around the ankle region of the CR spectrum for two primary particles (oxygen as well as proton) at zenith angles (0˚and 45˚).

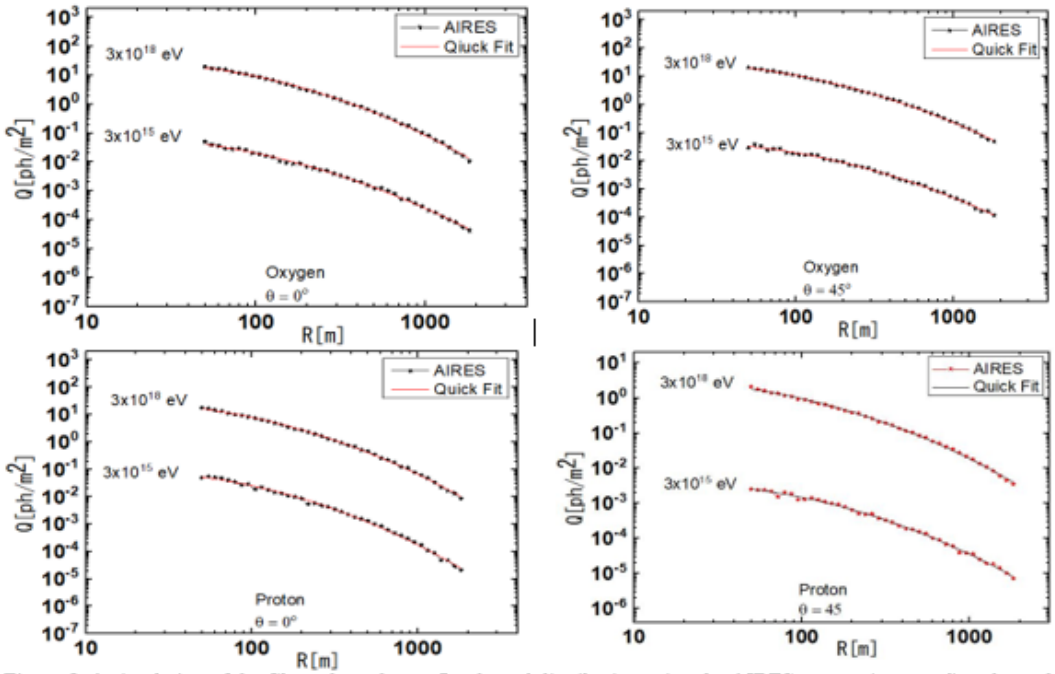

Figure 5: A simulation of the Cherenkov photon flux lateral distribution using the AIRES system (scattered) and one that was estimated Eq. (2) (solid lines) for oxygen as well as proton at two different zenith angles (0˚ and 45˚) and two different primary energies (3×10^{15} and 3×10^{18}) eV.

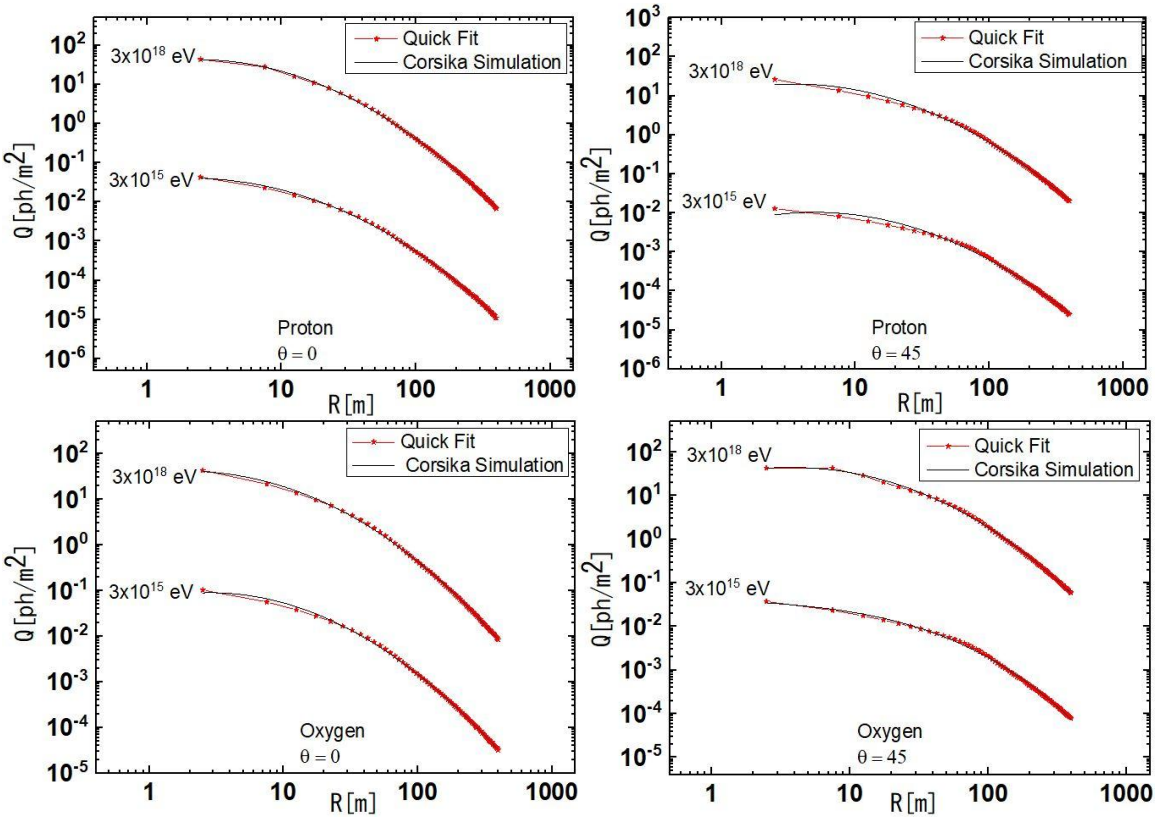

Figure 6: A lateral distribution simulation with the CORSIKA code (scattered) and one calculated with Eq. (2) (solid lines) for oxygen as will as proton at primary energies (3×10^{15} and 3×10^{18}) eV with two zenith angles (0˚ and 45˚).

Comparison of the Approximated LDF with Data Measurements

The discipline of cosmic ray astrophysics, which is dynamic and on the cutting edge of fundamental research, is studied by the Haverah Park EAS array. The Haverah Park array observable two primary goals are to investigate primary particle cascades in the atmosphere that are initiated by primary particles and to reconstruct the astrophysical characteristics of their origin, mass composition, energy spectrum, and primary intensity. Shower core position, azimuth and zenith angles, and individual LDF for Cherenkov photon flux $Q(R)$ are the primary factors in EAS observations. Figure 7 compares the approximate Cherenkov photon flux LDF obtained by Eq. 7 and 9 (quick function) with the Tunka EAS array for a primary proton with the energies (10^{15}, 10^{16}, 10^{18}, and 10^{19}) eV at the vertical shower at a distance of 100 to 400 m from the shower core to show the possibility of reconstructing the type of EAS primary particles.

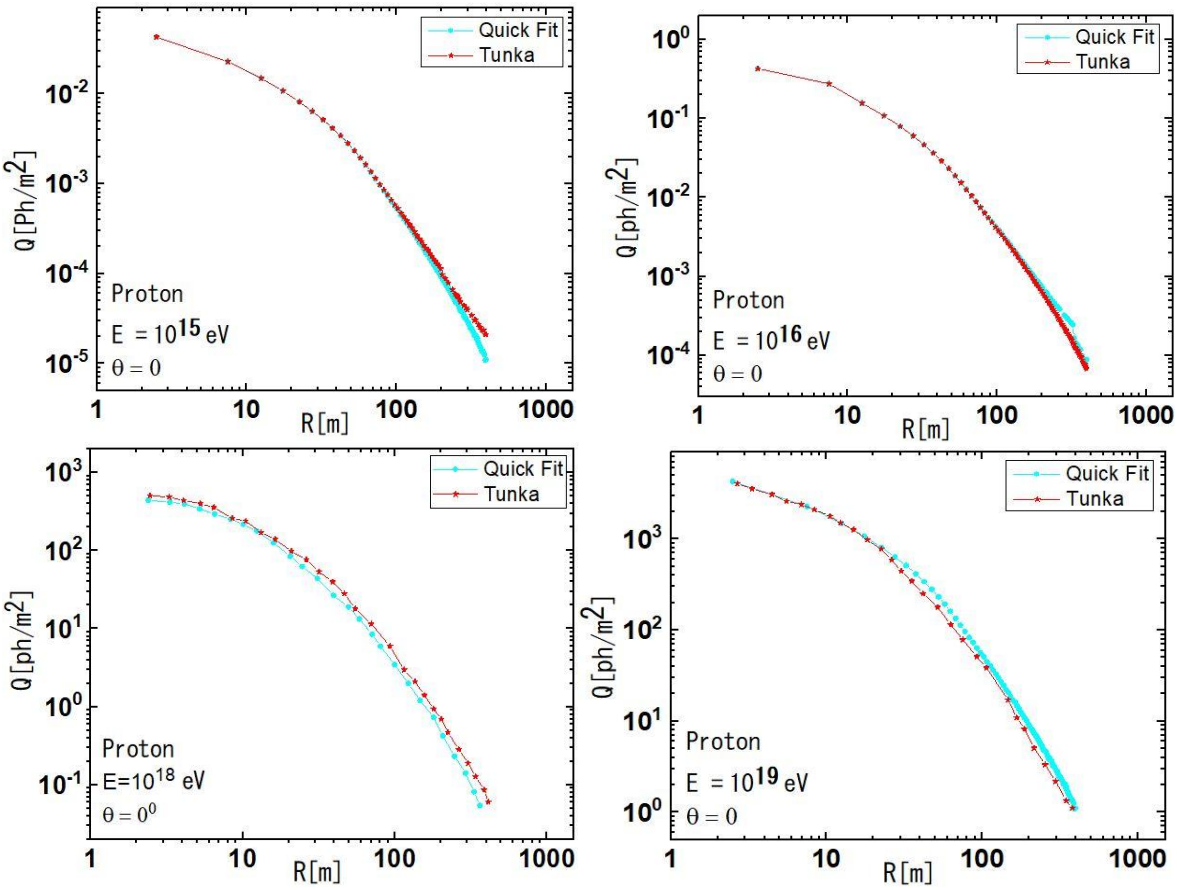

Figure 7: Comparison parameterized LDF obtained by (Quick Fit function) and the experimental data by Tunka [17] EAS array at 10^{15}, 10^{16}, 10^{18}, and 10^{19} eV for primary proton.

Conclusion:

The Cherenkov photon flux LDF from EAS particles that are started by the proton and primary oxygen simulations have been performed in the energy range between 10^{15} to 10^{19} eV by AIRES and CORSIKA code. Based on this simulation, which depended on the Quick Fit function, sets of approximation functions were created for two primary particles like oxygen as well as a proton, and zenith angles such as (0˚, 20˚, and 45˚) were also taken into account. By comparing the approximated Cherenkov photon flux LDF with that measured by the Tunka EAS array, it has been shown that it is possible to identify the particle responsible for EAS events and determine its energy around the knee and ankle areas of the cosmic ray spectrum. The results collected with AIRES and CORSIKA code are extrapolated for energies between 10^{15} and 10^{19} eV using the Cherenkov photon flux LDF parameterization. The primary advantage of the proposed approach is the possibility of rapidly creating a library of Cherenkov photon flux LDF patterns for use in analyzing detected actual events by the Haverah Park EAS array and to reconstruct a mass distribution as well as the energy spectrum of cosmic rays. The shower-to-shower fluctuation of the lateral distribution is very important, the dependences of lateral distribution on energy, mass, and zenith angle are different for different events. The study of EAS by the simulation through exponential function as a function of primary energy is the ability to determine the mass and energy of a primary particle.

References

[1] J. Espadanal and P. Gonçalves, "3D simulation for Cherenkov emissions in Extensive Air Showers," Feb. 2017, [Online]. Available: http://arxiv.org/abs/1702.03276

[2] W. S. Rada, A. C. Smith, T. R. Stewart, M. G. Thompson, and M. W. Treasure, "High-energy muons in extensive air showers," Nuovo Cim. A, vol. 54, no. 2, pp. 208–216, 1979, doi: 10.1007/BF02899788.

[3] A. A. Lagutin, R. I. Raikin, N. Inoue, and A. Misaki, "Electron lateral distribution in air showers: Scaling formalism and its implications," J. Phys. G Nucl. Part. Phys., vol. 28, no. 6, pp. 1259–1274, 2002, doi: 10.1088/0954-3899/28/6/309.

[4] A. Mishev, "Analysis of Lateral Distribution of Atmospheric Cherenkov Light at High Mountain Altitude Towards Event Reconstruction," ISRN High Energy Phys., vol. 2012, pp. 1–12, 2012, doi: 10.5402/2012/906358.

[5] A. A. Al-Rubaiee, "Extension of Cherenkov Light LDF Parametrization for Tunka and Yakutsk EAS Arrays," J. Astrophys. Astron., vol. 35, no. 4, pp. 631–638, 2014, doi: 10.1007/s12036-014-9305-x.

[6] L. Pentchev, P. Doll, and H. O. Klages, "The muon lateral distribution function as a transformation of the height-of-origin distribution in hadronic extensive air showers," J. Phys. G Nucl. Part. Phys., vol. 25, no. 6, pp. 1235–1248, 1999, doi: 10.1088/0954-3899/25/6/313.

[7] R. Ulrich, R. Engel, and M. Unger, "Hadronic multiparticle production at ultrahigh energies and extensive air showers," Phys. Rev. D - Part. Fields, Gravit. Cosmol., vol. 83, no. 5, 2011, doi: 10.1103/PhysRevD.83.054026.

[8] B. Bartoli et al., "EAS age determination from the study of the lateral distribution of charged particles near the shower axis with the ARGO-YBJ experiment," Astropart. Phys., vol. 93, pp. 46–55, 2017, doi: 10.1016/j.astropartphys.2017.06.003.

[9] I. Rasekh and D. Purmohammad, "On the estimation of the depth of maximum of extensive air showers using the steepness parameter of the lateral distribution of Cherenkov radiation," Astropart. Phys., vol. 132, 2021, doi: 10.1016/j.astropartphys.2021.102619.

[10] H.-J. Drescher and G. R. Farrar, "Dominant Contributions to Lateral Distribution Functions in Ultra-High Energy Cosmic Ray Air Showers," 2002, doi: 10.1016/S0927-6505(02)00203-7.

[11] S. C. Mavrodiev, A. L. Mishev, and J. N. Stamenov, "A method for energy estimation and mass composition determination of primary cosmic rays at the Chacaltaya observation level based on the atmospheric Cherenkov light technique," Nucl. Instruments Methods Phys. Res. Sect. A Accel. Spectrometers, Detect. Assoc. Equip., vol. 530, no. 3, pp. 359–366, 2004, doi: 10.1016/j.nima.2004.04.226.

[12] N. M. Budnev et al., "Tunka-133 EAS cherenkov array: Status of 2007," Proc. 30th Int. Cosm. Ray Conf. ICRC 2007, vol. 5, no. HE PART 2, pp. 973–976, 2007.

[13] M. Takeda et al., "Energy determination in the Akeno Giant Air Shower Array experiment," Astropart. Phys., vol. 19, no. 4, pp. 447–462, 2003, doi: 10.1016/S0927-6505(02)00243-8.

[14] S. J. Sciutto, "AIRES: A system for air shower simulations," 1999, doi: 10.13140/RG.2.2.12566.40002.

[15] L. Alexandrov, A. Mishev, and J. "Estimation of the primary cosmic radiation characteristics." *Proceedings of*

ICRC. Vol. 2001. No. 257. 2001.

[16] M. Ave, L. Cazón, J. A. Hinton, J. Knapp, J. Lloyd-Evans, and A. A. Watson, “Mass composition of cosmic rays in the range 2 × 10 17 -3 × 10 18 eV measured with the Haverah Park array,” Astropart. Phys., vol. 19, no. 1, pp. 61–75, 2003, doi: 10.1016/S0927-6505(02)00189-5.

[17] S. F. Berezhnev et al., "The Tunka-133 EAS Cherenkov light array: status of 2011." Nuclear Instruments and Methods in Physics Research Section A: accelerators, spectrometers, detectors and associated equipment 692 (2012): 98-105.

[18] S. K. Gupta et al., “GRAPES-3 - A high-density air shower array for studies on the structure in the cosmic-ray energy spectrum near the knee,” Nucl. Instruments Methods Phys. Res. Sect. A Accel. Spectrometers, Detect. Assoc. Equip., vol. 540, no. 2–3, pp. 311–323, 2005, doi: 10.1016/j.nima.2004.11.025.

[19] K. F. Fadhel and A. A. Al-Rubaiee, “Reconstruction of Air-Shower Parameters through Lateral Distribution Function of Ultra-High Energy Particles,” Acta Phys. Pol. A, vol. 140, no. 4, pp. 344–349, 2021, doi: 10.12693/APhysPolA.140.344.

[20] M. Risse, “Properties of extensive air showers,” Acta Phys. Pol. B, vol. 35, no. 6–7, pp. 1787–1797, 2004.

[21] T. Antoni et al., “Electron, muon, and hadron lateral distributions measured in air showers by the KASCADE experiment,” Astropart. Phys., vol. 14, no. 4, pp. 245–260, 2001, doi: 10.1016/S0927-6505(00)00125-0.

[22] A., Codino, & F. Plouin, (2009). Consequences of the common origin of the knee and ankle in Cosmic Ray Physics. Nuclear Physics B-Proceedings Supplements, 190, 228-239.

[23] A. A. Ivanov, S. P. Knurenko, and I. Y. Sleptsov, “Measuring extensive air showers with Cherenkov light detectors of the Yakutsk array: The energy spectrum of cosmic rays,” New J. Phys., vol. 11, 2009, doi: 10.1088/1367-2630/11/6/065008.

[24] A. Mishev, I. Angelov, E. Duverger, R. Gschwind, L. Makovicka, and J. Stamenov, “Experimental study and Monte Carlo modeling of the Cherenkov effect,” Nucl. Instruments Methods Phys. Res. Sect. A Accel. Spectrometers, Detect. Assoc. Equip., vol. 474, no. 2, pp. 101–107, 2001, doi: 10.1016/S0168-9002(01)00879-8.

[25] O. Saavedra and L. Jones, invited talk at Chacaltaya Meeting on Cosmic Ray Physics, La Paz, 23-27 July, (2000). Il Nuovo Cimento C vol. 24 July-October, (2001)

[26] S. C. Mavrodiev, A. L. Mishev, and J. N. Stamenov, “A method for energy estimation and mass composition determination of primary cosmic rays at the Chacaltaya observation level based on the atmospheric Cherenkov light technique,” *Nucl. Instruments Methods Phys. Res. Sect. A Accel. Spectrometers, Detect. Assoc. Equip.*, vol. 530, no. 3, pp. 359–366, 2004, doi: 10.1016/j.nima.2004.04.226.